The ^{129}Xe nuclear shielding tensor surfaces for Xe interacting with rare gas atoms

Cynthia J. Jameson[a] and Devin N. Sears
Department of Chemistry M/C-111, University of Illinois at Chicago, Chicago, Illinois 60607-7061

Angel C. de Dios
Department of Chemistry, Georgetown University, Washington, D.C. 20057-2222

(Received 9 September 2002; accepted 7 November 2002)

The shielding tensor surfaces for the Xe–Xe, Xe–Kr, Xe–Ar, and Xe–Ne dimers are calculated as a function of separation, using gauge-including atomic orbitals (GIAO) at the Hartree–Fock level, and also using density functional theory with the B3LYP hybrid functional. Since the highest quality potential energy functions are available for these systems, the available experimental data (temperature dependent second virial coefficients of the nuclear magnetic resonance chemical shifts) are from measurements on well-defined physical systems (Xe at low mole fraction in the gas phase), and the relation between the observed quantity and the shielding function is well-defined, these systems provide a means by which the dispersion component of the isotropic shielding function of Xe–Rg can be determined. The parallel component of the intermolecular shielding tensor is small and nearly independent of the method of calculation. Therefore, the dispersion component of the perpendicular component of the shielding function can be determined. © *2003 American Institute of Physics.* [DOI: 10.1063/1.1534093]

INTRODUCTION

The systems Xe–Xe, Xe–Kr, and Xe–Ar provide a means by which the electron correlation part of the intermolecular shielding response can be probed since the potential energy functions are accurately known, and the relation between theory and experiments (gas phase in the binary collision limit) is straightforward and simple. Since the supermolecule is very simple in these cases, the nature of the intermolecular shielding tensor can be examined in detail, i.e., $\sigma_{\perp}$ versus $\sigma_{\parallel}$, signs, magnitudes, dependence on collision partner. The shielding function for the particular system Xe–Xe is very relevant to the understanding of the observations of Xe chemical shifts in gas mixtures, in homogeneous solutions, and in heterogeneous systems in which the ^{129}Xe nucleus is being used as a probe of internal confined spaces, in porous aluminosilicate and other inorganic materials, in biological systems, even in tissues, and in organic polymers, crystalline, amorphous or liquid crystalline.[1,2] With the increasing use of optically pumped Xe, so-called hyperpolarized ^{129}Xe, particularly for enhanced sensitivity of Xe in cavities of proteins and other biological environments, and for development of ^{129}Xe as a biosensor,[3,4] as well as for direct monitoring of structural changes and nanoporosity,[5,6] detailed understanding of the Xe intermolecular chemical shift tensor has become very important.

METHOD

Shielding calculations have reached a reasonable level of accuracy for many applications.[7,8] In particular, we examine intermolecular ^{129}Xe shielding in rare gas pairs. In a comparative study of Ne–Ne shielding,[8] using different combinations of density functionals (VWN, BPW91, BLYP, B3LYP) and also Hartree–Fock, and coupled cluster singles and doubles with triplet excitations, CCSD(T), it was found that all the calculated tensors as a function of Ne–Ne distance, except for the VWN functional, are very close to the CCSD(T) result which is considered the benchmark in shielding studies. All the gradient-corrected functionals used performed quite well, and the hybrid B3LYP functional performed best. The shape of the shielding function is correctly reproduced by all, with the Hartree–Fock giving consistently more shielded values and the density functional theory (DFT) methods giving consistently more deshielded values than the most accurate CCSD(T) results. It would not be surprising to find the trends found for Ne–Ne to hold also for ^{129}Xe shielding in Xe-rare gas dimers. We report here two sets of calculations of ^{129}Xe shielding in Xe–Xe, Xe–Kr, Xe–Ar, and Xe–Ne dimers over a wide range of separations, one at the Hartree–Fock level, and the other using DFT-B3LYP as a representative of DFT methods. The same basis sets were used in both methods. B3LYP is one of Becke's three-parameter hybrid functionals that uses the correlation functional from Lee, Yang, and Parr,[9] and a fraction of the Becke exchange functional[10] is replaced by exact Hartree–Fock exchange, according to the recipe by Becke.[11] It is one of the popularly tested functionals in DFT calculations, and we choose it based on best demonstrated performance in Ne–Ne in comparison with other functionals. For Xe atom we use 240 basis functions, including *f* orbitals, the same basis set as we had used earlier and described in Ref. 12, from the compilation by Partridge and Faegri, with additional polarization functions from Bishop and Cybulski.[13,14] The basis sets used for other rare gas atoms, also taken form

[a]Electronic mail: cjj@sigma.chem.uic.edu

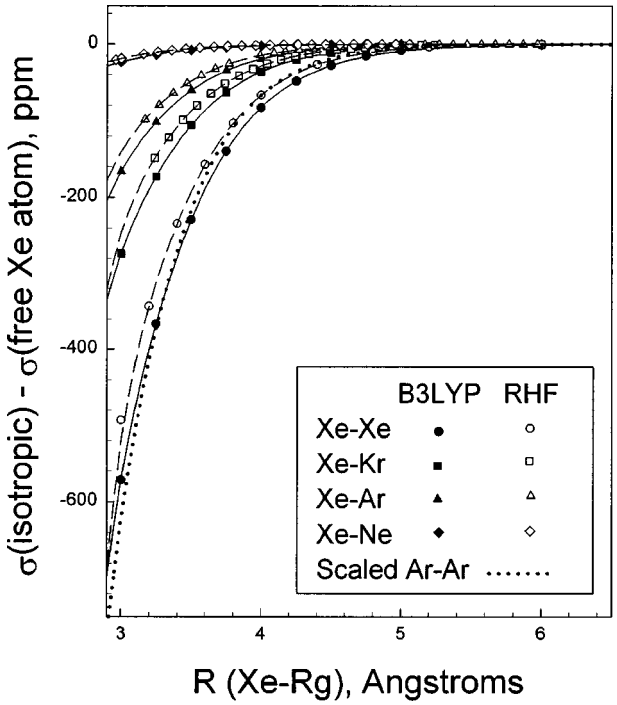

FIG. 1. The isotropic ^{129}Xe shielding for the Xe–Rg dimer, calculated at the Hartree–Fock level and at a correlated level using DFT method with the B3LYP hybrid functional. The curves are the results of fitting the calculated shieldings to a sum of inverse powers of the separation, as in Eq. (1). The Xe–Xe shielding previously used by us is the scaled Ar–Ar shielding function, also shown here for comparison.

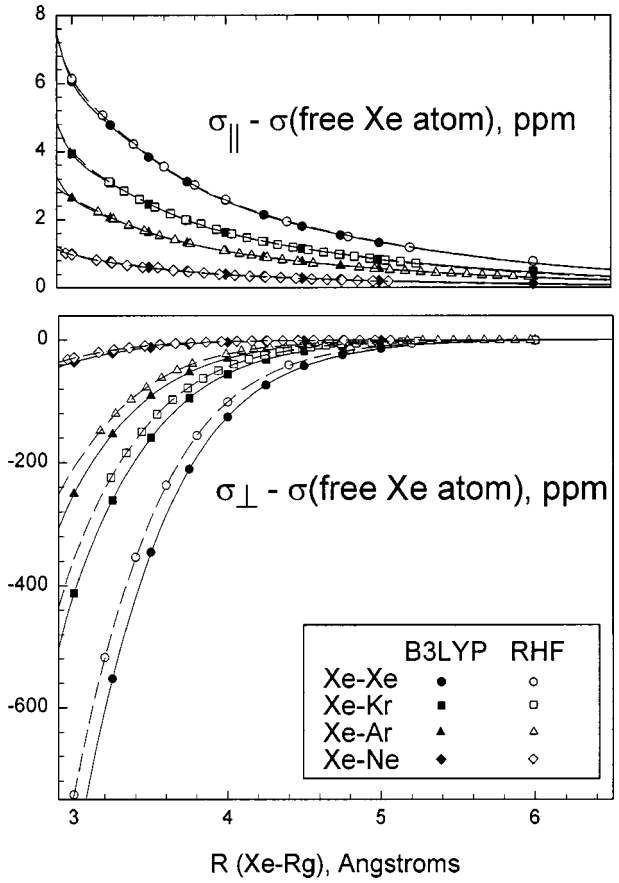

FIG. 2. The perpendicular and the parallel components of the ^{129}Xe shielding tensor for the Xe–Rg dimer, calculated at the Hartree–Fock level and at a correlated level using DFT method with the B3LYP hybrid functional. The curves are the results of fitting the calculated shieldings to a sum of inverse powers of the separation, as in Eq. (1). Note the huge difference in scale used in plotting the shielding components.

the Partridge and Faegri compilation, are as follows: for Kr, 128 functions consisting of uncontracted $(21s16p10d)$ plus *s*, *p*, and *d* polarization functions; for Ar, 85 basis functions, uncontracted $(20s15p0d)$ plus four *d* polarization functions, for Ne, 77 basis functions, uncontracted $(18s13p0d)$ plus four *d* polarization functions.[13] Distributed gauge origins are implemented through the use of gauge-including atomic orbitals,[15] and the GAUSSIAN 98 program package was used for all calculations.[16] Counterpoise calculations were performed at several distances in order to correct for basis set superposition errors.[17] $\sigma(\infty)$ is the shielding calculated using all the basis functions, but with only the electrons on the Xe atom, the absolute shielding of the free Xe atom under full counterpoise correction. In all cases, the counterpoise corrections were found to be negligibly small, for example, 0.0010 ppm for Xe–Ne at 3.76 Å, where $\sigma(R)-\sigma(\infty)=-2.7521$ and 0.0079 ppm for Xe–Kr at 4.14 Å, where $\sigma(R)-\sigma(\infty)=-20.1702$ ppm, indicating that the basis set we are using for Xe is large enough.

RESULTS

The isotropic shielding response for ^{129}Xe in Xe atom as a function of internuclear separation is shown in Fig. 1 for Xe–Xe, Xe–Kr, Xe–Ar, and Xe–Ne dimers. In every case, the DFT-B3LYP results are more deshielded over the entire range of distances, in comparison with the results at the *ab initio* Hartree–Fock level. This was found also to be the case for Ne–Ne, where the benchmark calculations at the CCSD(T) level are available for comparison.[8] Upon approach of the Ne atom, the Hartree–Fock results for $[\sigma(R_{\mathrm{Ne-Ne}})^{\mathrm{HF}}-\sigma(\infty)]$ are less deshielded and the DFT results are more deshielded than the CCSD(T) results.

The values calculated in the present work are well described by a function in inverse powers of distance, of the form

$$\sigma_{\mathrm{iso}}(R)-\sigma(\infty)=\mathrm{C}_6R^{-6}+\mathrm{C}_8R^{-8}+\mathrm{C}_{10}R^{-10}+\mathrm{C}_{12}R^{-12}+\mathrm{C}_{14}R^{-14}. \quad (1)$$

For the isotropic shielding, these functions are shown as curves in Fig. 1, together with the *ab initio* values at the Hartree–Fock level and the values at the DFT-B3LYP level. Figure 2 shows the individual tensor components perpendicular and parallel to the line of centers, $\sigma_{\perp}(R)-\sigma(\infty)$, and $\sigma_{\parallel}(R)-\sigma(\infty)$, and the curves that are the results of fitting the values of the individual components to the same form as Eq. (1). We note how the components of the tensor change with separation: The parallel component is diamagnetic, increasing slightly with decreasing distance, and essentially independent of the computational method used. In fact, the Flygare approximation[18,19] gives a reasonable accounting of this component, as has been demonstrated in Fig. 4 of Ref. 20. On the other hand, the component perpendicular to the

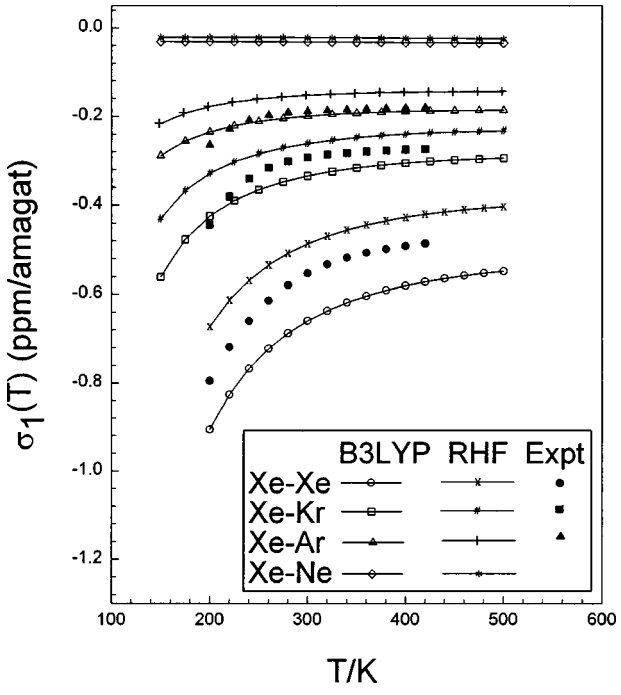

FIG. 3. The density coefficient of the ^{129}Xe shielding for Xe at infinite dilution in Rg gas, calculated from the shielding functions obtained at the Hartree–Fock level and from the DFT-B3LYP method, using Eq. (2) and the best available potential functions from Aziz *et al.* (Refs. 21–23). The experimental values from Jameson *et al.* (Ref. 24) are shown for comparison.

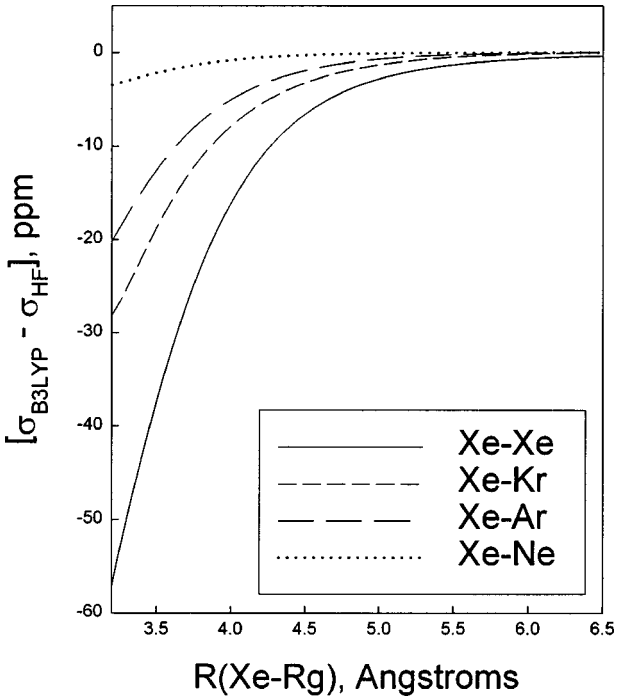

FIG. 4. The differences between the isotropic ^{129}Xe shielding for the Xe–Rg dimer, calculated at a correlated level using DFT/B3LYP and at the Hartree–Fock level, provide the relative magnitudes of the correlation contribution to intermolecular shielding.

line of centers, $\sigma_{\perp}(R)-\sigma(\infty)$, is deshielded at all distances and is found to be consistently somewhat more deshielded when calculated using DFT-B3LYP than when using Hartree–Fock.

The density coefficient of the shielding, the so-called second virial coefficient of the shielding can be calculated using the intermolecular potential functions which are well-known for the rare gas pairs from the work of Aziz *et al.*[21–23] using

$$\sigma_1(T)=4\pi\int_0^{\infty}[\sigma_{\mathrm{iso}}(R)-\sigma(\infty)]\exp[-V(R)/kT]R^2dR. \quad (2)$$

In Fig. 3 are the density coefficients $\sigma_1(T)$ calculated from the Hartree–Fock and DFT-B3LYP results for Xe–Xe, Xe–Kr, Xe–Ar, together with the predictions for Xe–Ne. Comparison of calculated $\sigma_1(T)$ against experimental density coefficients from Jameson *et al.*[24] in Fig. 3 show that the predictions at the Hartree–Fock level, which account correctly for the exchange, are somewhat shy of experiments. On the other hand, the DFT method using the B3LYP hybrid functional overshoots the experiments somewhat. In going from Xe–Xe to Xe–Kr to Xe–Ar, the difference between the Hartree–Fock and DFT-B3LYP shielding function leads to a decreasing fraction of the observed density coefficient: $\{[\sigma_1(300\ \mathrm{K})_{\mathrm{B3LYP}}-\sigma_1(300\ \mathrm{K})_{\mathrm{HF}}]/\sigma_1(300\ \mathrm{K})_{\mathrm{Expt.}}\}$ is 0.143 for Xe–Xe, 0.115 for Xe–Kr, and 0.044 for Xe–Ar. Although calculations at the DFT/B3LYP do not provide the accuracy that one can get from full configuration interaction or coupled cluster calculations (CCSDT), the differences between the ^{129}Xe shielding functions $[\sigma(R)^{\mathrm{B3LYP}}-\sigma(R)^{\mathrm{HF}}]$, shown in Fig. 4, do provide a measure of the relative magnitudes of the correlation contributions to intermolecular shielding. Three very clear trends are that the correlation contributions to intermolecular shielding (a) are deshielding, (b) do decrease in going from Xe to Ne as the interacting partner, and (c) do decrease with increasing distance.

DISCUSSION

In our earlier work, we had found that the intermolecular shielding in the various light rare gas pairs scaled to one another with fundamental factors $\langle a_0^3/r^3\rangle\cdot\alpha(0)$ for the atom whose shielding is being considered, e.g., Xe, and with factors $\alpha_{\mathrm{Rg}}(0)\cdot[\mathrm{IP}_{\mathrm{Xe}}\times\mathrm{IP}_{\mathrm{Rg}}/(\mathrm{IP}_{\mathrm{Xe}}+\mathrm{IP}_{\mathrm{Rg}})]$, with the distances scaled to r_0 of the potential function, for the interacting rare gas pair.[20] From this discovered scaling, we found Xe–Xe, Xe–Kr, and Xe–Ar shielding functions from scaling the Ar–Ar shielding function. In Fig. 1 we show a comparison with the previously used Xe–Xe shielding function in our early work,[25–32] obtained by scaling to Xe–Xe from LORG calculations of Ar shielding in Ar–Ar.[20] We see that the scaled Ar–Ar function was not that bad, considering the basis set used for Ar was not as extensive as the 240 basis functions we now use for Xe atom.

In the early modeling of intermolecular shifts, Raynes, Buckingham, and Bernstein (RBB) proposed contributions to the shielding that included bulk susceptibility, electrical, magnetic anisotropy, and dispersion contributions,[33]

$$\sigma(R)=\sigma_{\mathrm{bulk}}+\sigma_E+\sigma_m+\sigma_W.$$

For rare gas pairs, there are no electrical or magnetic anisotropy terms, so that the RBB model would have only dispersion contributions, which were considered to be approximated by the form $-B\langle F^2\rangle$. That is, the RBB model for the dispersion contributions to Xe shielding is the nonvanishing average of the square of the fluctuating electric fields associated with dispersion interactions between Xe and the collision partner. B is the same parameter associated with any electric field terms for Xe, that is, B is the second derivative of the shielding with respect to the external electric field. The problem with this model is that no single value of the B parameter could account for the observed density coefficient $\sigma_1(T)$ of the Xe shielding as a function of temperature for Xe–Rg. Furthermore, the value of B has since been calculated for Xe atom in a uniform external electric field[14] and it is found to be too small to account for the order of magnitudes of the density coefficients $\sigma_1(T)$ that were observed experimentally for Xe in the gas phase. We have since established that a significant part of the intermolecular shielding observed experimentally could be accounted for entirely by overlap and exchange, from *ab initio* calculations not including any electron correlation.[20]

In the present work, the calculations of the Xe shielding in Xe–Xe, Xe–Kr, Xe–Ar dimers at the Hartree–Fock level, using basis sets large enough so that the counterpoise corrections to the shielding are negligible, provide shielding functions $\sigma(R)$ that include no dispersion contributions at all, yet can account to a great extent for the observed $\sigma_1(T)$ in the gas phase, as shown in Fig. 3. Therefore, overlap and exchange are responsible to a predominant degree, for the observed intermolecular chemical shifts of Xe. Nevertheless, we wish to determine what fraction of the shielding response at a given internuclear separation can be attributed to electron correlation? For which component ($\sigma_\perp$ component?) is the electron correlation significant (in absolute terms, in relative terms)? What fraction of the observed density coefficient $\sigma_1(T)$ can be attributed to electron correlation?

First of all, we find that the parallel component $\sigma_\parallel$ along the line of centers has a negligible electron correlation contribution (see Fig. 2). To determine electron correlation contributions to $\sigma(R)$, we will assume that the potential energy functions for rare gas are perfect and the experimental values of the density coefficients of the Xe chemical shift as a function of temperature are reliable. Knowing that the Hartree–Fock method gives correct exchange, we will attribute the difference between the shielding function $\sigma(R)$ that provides the observed $\sigma_1(T)$ and that $\sigma(R)$ calculated at the Hartree–Fock level, to the electron correlation contribution to shielding. We find that, for Xe in Xe–Xe, we need to add 15% to the $\sigma(R_{\mathrm{Xe-Xe}})^{\mathrm{HF}}$ to account for the missing electron correlation contribution. Similarly, for the Xe in Xe–Kr, we need to add 10%. That is, the recommended $\sigma(R)$ shielding functions are 1.1505 $\sigma(R_{\mathrm{Xe-Xe}})^{\mathrm{HF}}$ and 1.1021 $\sigma(R_{\mathrm{Xe-Kr}})^{\mathrm{HF}}$, respectively. In the case of Xe in Xe–Ar, it appears that we need to add 23.6%. However, a consideration of the experimental details lead us to place a larger error bar on this factor than on the Xe–Xe and Xe–Kr systems. The observed Xe shielding change relative to the free Xe atom in a mixture of Xe and Ar gas is due to the sum $\sigma_{1\mathrm{Xe-Xe}}(T)\cdot\rho_{\mathrm{Xe}}+\sigma_{1\mathrm{Xe-Ar}}(T)\cdot\rho_{\mathrm{Ar}}$ in the limit of linear dependence on densities. In principle the Xe–Xe contribution can be subtracted out completely as the $\sigma_{1\mathrm{Xe-Xe}}(T)\cdot\rho_{\mathrm{Xe}}$ term, which is well known form measurements in pure xenon gas. A practical number of Xe atoms in the sample for nuclear magnetic resonance (NMR) detection means that there is always some $\sigma_{1\mathrm{Xe-Xe}}(T)\cdot\rho_{\mathrm{Xe}}$ correction to be made in each mixed rare gas sample. Since $|\sigma_{1\mathrm{Xe-Xe}}(T)|$ is considerably larger than $|\sigma_{1\mathrm{Xe-Ar}}(T)|$, errors in Xe densities leading to incomplete subtraction of the Xe–Xe contribution, lead to larger relative errors associated with determination of $\sigma_{1\mathrm{Xe-Ar}}(T)$. The relative errors would be much worse for Xe–Ne mixtures. The B3LYP calculations overshoot in every case, although they do get closer to the correct values as the rare gas partner of the Xe becomes smaller. For example, $\sigma(R)$ shielding functions that would reproduce the $\sigma_1(T=300\ \mathrm{K})$ are 0.85 $\sigma(R_{\mathrm{Xe-Xe}})^{\mathrm{B3LYP}}$, 0.87 $\sigma(R_{\mathrm{Xe-Kr}})^{\mathrm{B3LYP}}$, and 0.94 $\sigma(R_{\mathrm{Xe-Ar}})^{\mathrm{B3LYP}}$, with larger uncertainty in the Xe–Ar case, for reasons already discussed. Figure 4 leads us to conclude that in absolute terms, the electron correlation contributions to shielding decrease in magnitude in going from Xe–Xe to Xe–Kr to Xe–Ar. We assume that Xe–Ne will be in the right place in this sequence, since the difference between the HF and B3LYP results is smaller yet, although we have no experimental $\sigma_1(T)$ values to use as a direct measure in this case. Experimental $\sigma_1(T)$ data show that for Xe–Kr and Xe–Xe the contributions are about half of the $[\sigma(R_{\mathrm{Xe-Rg}})^{\mathrm{B3LYP}}-\sigma(R_{\mathrm{Xe-Rg}})^{\mathrm{HF}}]$ in Fig. 4. We recommend that a better estimate of the electron correlation contributions to Xe–Ar shielding, instead of experiment, is that provided by half the difference between the B3LYP and HF shielding functions, i.e., $\sigma(R_{\mathrm{Xe-Rg}})\approx 1.15\sigma(R_{\mathrm{Xe-Xe}})^{\mathrm{HF}}$.

Corresponding-states-scaling of the shielding function discovered from LORG calculations of various rare gas pairs such as Ar–Ar, Ar–Ne, Ne–Ne,[20] is found here again to be valid. The scaling factor, for shielding of the same rare gas atom, Xe, with various partners Rg, as has been suggested at that time,[20] assumed the shielding function is proportional to $\alpha_{\mathrm{Rg}}(0)\cdot[\mathrm{IP_{Xe}}\times\mathrm{IP_{Rg}}/(\mathrm{IP_{Xe}}+\mathrm{IP_{Rg}})]$, with the distances scaled to r_0 of the potential function, i.e., when the shielding functions are expressed in inverse powers of (R/r_0). Corresponding-states-scaling of the rare gas density coefficients of the shielding is possible by using reduced temperatures. In Figs. 4 and 5 we show the contributions to the density coefficients, $\sigma_1(T)$, from various regimes of the intermolecular separation; we display the integrand in $\sigma_1(T)=\int_0^\infty$ (Integrand) dR in order to show which parts of the potential surface are responsible for the observed density dependence of the ^{129}Xe NMR signal. The correspondence becomes apparent when we express the separations in terms of R/r_0, the temperatures as reduced temperature T/T_c, and we scale the integrand with the scaling factor $\{[\alpha_{\mathrm{Xe}}(0)/\alpha_{\mathrm{Rg}}(0)\cdot[\mathrm{IP_{Xe}}/\mathrm{IP_{Rg}}]\cdot[(\mathrm{IP_{Xe}}+\mathrm{IP_{Rg}})/2\mathrm{IP_{Xe}}]\}$. We see in Fig. 5, despite the large deshielding that occurs at very short distances (as shown in Fig. 1), nothing of the ^{129}Xe shielding function for separations inside of $0.85r_0$ contributes at $T/T_c=1.0$ for Xe–Xe, Xe–Kr, Xe–Ar. In Fig. 5 we see a correspondence of the regimes of separation, as well as a correspondence of the magnitudes of the integrand that con-

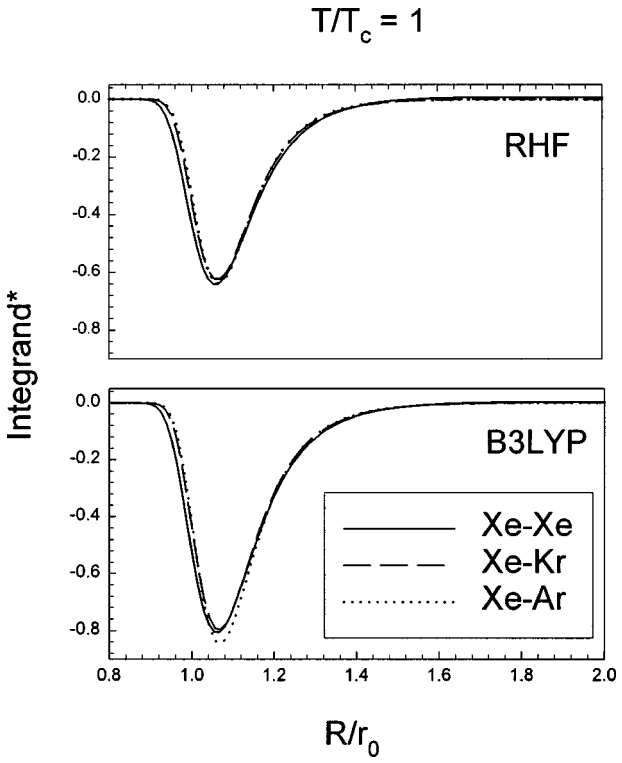

FIG. 5. Contributions to $\sigma_1(T=T_c)$ from various Xe–Rg separations. Integrand* stands for scaled values using the scaling factor $\{[\alpha_{Xe}(0)/\alpha_{Rg}(0)]\cdot[IP_{Xe}/IP_{Rg}]\cdot[IP_{Xe}+IP_{Rg})/2IP_{Xe}]\}$, where $\sigma_1(T)=\int_0^\infty$ (integrand) dR.

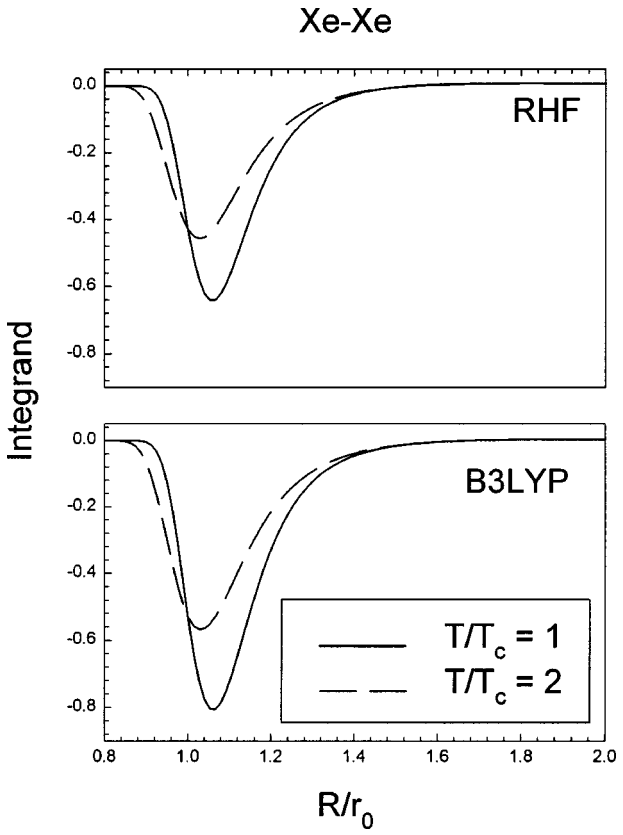

FIG. 6. Contributions to $\sigma_1(T)$ from various Xe–Xe separations, at two reduced temperatures. Definitions are as given in Fig. 5.

tribute to the density coefficients. Therefore, one expects also a correspondence of the observed density coefficient of shielding. The possibility of a correspondence has already been noted in the early (1975) interpretations of the experimental observations,[24] although the potential functions available at that time, even for the rare gas pairs, were not very good; and the correspondence could not clearly be established for the observed $\sigma_1(T)$ values, since the shielding functions were of unknown form at that time. Figure 5 provides a unified view of the intermolecular shielding leading to the density dependent chemical shift for all Xe–Rg pairs.

The temperature dependence of the density coefficients for Xe–Xe are seen in Fig. 6. As the temperature increases, the shielding functions are explored farther into the repulsive region of the potential. For Xe–Xe, hardly any of the shielding function at separations inside the $0.80r_0$ contributes at $T/T_c=2.0$, as seen in Fig. 6. By virtue of the near-coincidence of the scaled curves (seen in Fig. 5) for the rare-gas pairs, the resulting general decrease in the magnitude of the density coefficient with increasing temperature is clearly seen here for all Xe–Rg pairs.

The electron density change upon dimer formation may offer a general qualitative understanding of intermolecular shifts in the absence of hydrogen bonding or other partly covalent interactions. In other words, can one understand the large Xe shielding response by examining the electron density difference maps? Electron density difference maps resulting from the B3LYP calculations in the Xe–Xe dimer are shown in Fig. 7 for distances 4.5 (top) and 3.5 Å (bottom). We had anticipated a tendency toward spherical-to-prolate at long distances and spherical-to-oblate at short distances. The results show that the electron density changes are more complicated and do not lend themselves to such oversimplified descriptions. In any case, the deviations from spherical sym-

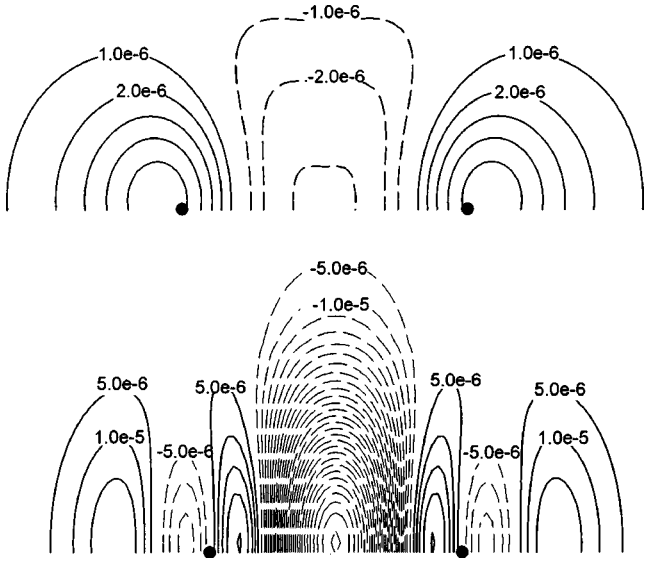

FIG. 7. Contours of the electron density changes (relative to the unperturbed Xe atoms) for Xe_2 at a separation of 4.5 Å (top) and 3.5 Å (bottom), taken from the B3LYP calculations. The dashed lines correspond to depletion of electron density. Contours are separated by $1.0\times10^{-6}e$ for the 4.5 Å distance and $0.5\times10^{-5}e$ for the 3.5 Å. Nuclear positions are indicated by the filled circles.

metry of the electron distribution of the Xe atom, caused by the close approach of another Xe atom, leads to nonvanishing paramagnetic shielding.

CONCLUSION

We have found that the intermolecular shielding $[\sigma(R) - \sigma(\infty)]$ for rare gas pairs predominantly arises from overlap and exchange, but the electron correlation contribution is not insignificant. The recommended shielding functions are $1.1505[\sigma(R_{\mathrm{Xe-Xe}})^{\mathrm{HF}} - \sigma(\infty)]$, $1.1021[\sigma(R_{\mathrm{Xe-Kr}})^{\mathrm{HF}} - \sigma(\infty)]$, and $1.15[\sigma(R_{\mathrm{Xe-Ar}})^{\mathrm{HF}} - \sigma(\infty)]$. In other words, the contribution of electron correlation to ^{129}Xe intermolecular shielding in Xe–Xe is 15%, in Xe–Kr is 10%, in Xe–Ar is 15%. In absolute terms, the electron correlation contributions to intermolecular ^{129}Xe shielding decreases in magnitude in going from Xe–Xe, to Xe–Kr, to Xe–Ar, to Xe–Ne. The component of the shielding tensor parallel to the line of centers is entirely diamagnetic, and is essentially independent of the method of calculation, having insignificant electron correlation contributions. On the other hand, the perpendicular component is primarily a paramagnetic deshielding, and has electron correlation contributions that are not insignificant. Consideration of corresponding states leads us to a unified view of the contributions of shielding at various internuclear separations to the Xe intermolecular shielding observed in rare gas mixtures. We find a correspondence of the regimes of separations, as well as a correspondence of the magnitudes of the integrand that contribute to the density coefficients.

ACKNOWLEDGMENT

The support of this research by the National Science Foundation (Grant No. CHE99-79259) is gratefully acknowledged.

[1] J. L. Bonardet, J. Fraissard, A. Gedeon, and M. A. Springuel-Huet, J. Catal. Rev. Sci. Eng. **41**, 115 (1999).
[2] C. I. Ratcliffe, Annu. Rep. NMR Spectrosc. **36**, 123 (1998).
[3] M. M. Spence, S. M. Rubin, I. E. Dimitrov, E. J. Ruiz, D. E. Wemmer, A. Pines, S. Q. Yao, F. Tian, and P. G. Schultz, Proc. Natl. Acad. Sci. U.S.A. **98**, 10654 (2001).
[4] C. R. Bowers, V. Storhaug, C. E. Webster, J. Bharatam, A. Cottone III, R. Gianna, K. Betsey, and B. J. Gaffney, J. Am. Chem. Soc. **12**, 9370 (1999).
[5] A. V. Nossov, D. V. Soldatov, and J. A. Ripmeester, J. Am. Chem. Soc. **123**, 3563 (2001).
[6] I. L. Moudrakovski, A. A. Sanchez, C. I. Ratcliffe, and J. A. Ripmeester. J. Phys. Chem. B **105**, 12338 (2001).
[7] *Modeling NMR Chemical Shifts. Gaining Insights into Structures and Environment*, edited by J. C. Facelli and A. C. de Dios, ACS Symposium Series Vol. 732 (Oxford University Press, Oxford, 1999).
[8] M. Bühl, M. Kaupp, O. L. Malkina, and V. G. Malkin, J. Comput. Chem. **20**, 91 (1999).
[9] C. Lee, W. Yang, and R. G. Parr, Phys. Rev. B **37**, 785 (1988).
[10] A. D. Becke, Phys. Rev. A **38**, 3098 (1988).
[11] A. D. Becke, J. Chem. Phys. **98**, 5648 (1993).
[12] A. C. de Dios and C. J. Jameson, J. Chem. Phys. **107**, 4253 (1997).
[13] H. Partridge and K. Faegri, Jr., NASA Technical Memorandum 103918 (1992).
[14] D. A. Bishop and S. M. Cybulski, Chem. Phys. Lett. **211**, 255 (1993).
[15] K. Wolinkski, J. F. Hinton, and P. Pulay, J. Am. Chem. Soc. **112**, 8251 (1990).
[16] M. J. Frisch, G. W. Trucks, H. B. Schlegel *et al.*, GAUSSIAN 98, Revision A.9, Gaussian, Inc., Pittsburgh, PA, 1998.
[17] S. F. Boys and F. Bernardi, Mol. Phys. **19**, 538 (1970).
[18] T. D. Gierke and W. H. Flygare, J. Am. Chem. Soc. **94**, 7277 (1972).
[19] W. H. Flygare and J. Goodisman, J. Chem. Phys. **49**, 3122 (1968).
[20] C. J. Jameson and A. C. de Dios. J. Chem. Phys. **97**, 417 (1992).
[21] R. A. Aziz and M. J. Slaman, Mol. Phys. **57**, 825 (1986).
[22] R. A. Aziz and A. van Dalen, J. Chem. Phys. **78**, 2402 (1983).
[23] D. A. Barrow, M. J. Slaman, and R. A. Aziz, J. Chem. Phys. **91**, 6348 (1989).
[24] C. J. Jameson, A. K. Jameson, and S. M. Cohen, J. Chem. Phys. **62**, 4224 (1975).
[25] C. J. Jameson, A. K. Jameson, B. I. Baello, and H. M. Lim. J. Chem. Phys. **100**, 5965 (1994).
[26] C. J. Jameson, A. K. Jameson, H. M. Lim, and B. I. Baello, J. Chem. Phys. **100**, 5977 (1994).
[27] C. J. Jameson, A. K. Jameson, R. E. Gerald II, and H.-M. Lim, J. Chem. Phys. **103**, 8811 (1995).
[28] C. J. Jameson, A. K. Jameson, and H. M. Lim, J. Chem. Phys. **104**, 1709 (1996).
[29] C. J. Jameson and H. M. Lim, J. Chem. Phys. **107**, 4373 (1997).
[30] C. J. Jameson, A. K. Jameson, and H. M. Lim, J. Chem. Phys. **107**, 4364 (1997).
[31] C. J. Jameson, H. M. Lim, and A. K. Jameson, Solid State Nucl. Magn. Reson. **9**, 277 (1997).
[32] C. J. Jameson, A. K. Jameson, P. Kostikin, and B. I. Baello, J. Chem. Phys. **112**, 323 (2000).
[33] W. T. Raynes, A. D. Buckingham, and H. J. Bernstein, J. Chem. Phys. **36**, 3481 (1962).